# Assessing the uncertainty of soil moisture impact on convective precipitation using a new ensemble approach

Olga Henneberg[1], Felix Ament[2], and Verena Grützun[2]

[1]Institute for Atmospheric and Climate Science, ETH Zurich
[2]Meteorological Institute, University of Hamburg

*Correspondence to:* Olga Henneberg (olga.henneberg@alumni.ethz.ch)

**Abstract.** Soil moisture influences the occurrence of convective precipitation. Therefore, ~~an~~ accurate knowledge about soil moisture might be useful for an improved prediction of convective cells. However, simulations with slightly changed model setup cause a large spread in model results that result from the chaotic behaviour of the atmospheric system and stochastic variability. By shifting the model domain, an estimate on the uncertainty of the model results can be calculated. This uncertainty estimate, which includes ten simulations with shifted model boundaries, is compared to the effects caused by soil moisture on precipitation. With this approach the effect if soil moisture is quantified.

We performed seven experiments with modified soil moisture to address the effect of soil moisture on precipitation. Each of the experiments consists of ten ensemble members. In three out of the seven experiments precipitation changes exceed the model spread in either amplitude, location or structure. This changes are caused by a 50% soil moisture enhancement in either the whole or part of the model domain or dry-out of the whole model domain. Enhanced or reduced soil moisture predominately result in reduced precipitation rates. Replacing the soil moisture by a realistic field from different days has an insignificant influence on the precipitation. We point out the need for uncertainty estimates in real-case soil moisture studies.

## 1 Introduction

Convective precipitation changes rapidly in time and is very variable in space (Pedersen et al., 2010). The heterogeneity of convective precipitation and the interaction of different scales challenge atmospheric models on the global and regional scale. Nowadays regional climate models operate with a horizontal resolution of $1\,\mathrm{km}$ and can represent convective processes explicitly to improve weather forecast (Mass et al., 2002). Nevertheless, precipitation formation results from a complex chain of atmospheric processes, which range from the microscale to the synoptic scale (Richard et al., 2007). Because many of these processes remain unresolved, precipitation states a highly uncertain quantity. Soil moisture sits at the beginning of convective precipitation formation.

Soil moisture affects the partitioning of turbulent heat fluxes into sensible and latent heat, what affects the surface and boundary layer temperature and the humidity in the lower boundary layer. The surface temperature plays a crucial role in the initiation of convection, whereas the specific water content in the boundary layer modifies moist conditional instability. On the one hand, high surface temperatures initiate convection with a low soil moisture content. On the other hand, high soil moisture can

destabilise the atmosphere by introducing water vapour in the lower troposphere what also favours convection. Conclusively moistening and drying of the lower boundary can intensify precipitation and vice versa. Whereas, a strong systematic effect on soil moisture changes exists for the latent and sensible heat fluxes, as well as equivalent potential temperature, lifting condensation level and convective energy, that follow the process chain (Barthlott et al., 2011). Despite to the systematic effect on partitioning of the heat fluxes, precipitation reacts less systematically on soil moisture variations (Barthlott and Kalthoff, 2011; Hohenegger et al., 2009). Furthermore, the distribution and inhomogeneity of soil moisture patterns may initiate secondary circulation (Clark et al., 2004; Adler et al., 2011; Kang and Bryan, 2011; Dixon et al., 2013; Maronga and Raasch, 2013; Froidevaux et al., 2014).

There is no clear agreement on soil moisture precipitation interaction in the literature: Barthlott et al. (2011) found a strong dependency of precipitation, with changes larger than 500%, for a soil moisture variation of $\pm 25\%$ in regions with low mountain ranges, and changes of up to $-75\%$ for domains with higher mountain ranges. They could not identify significant differences between planetary boundary driven, and synopticaly forced, conditions. Hauck et al. (2011) determined large systematic differences between modelled and observed soil moisture. The influence on simulated precipitation in their study was complex and depended strongly on the chosen case and domain. A dependency of all convective indices on the equivalent potential temperature was found by Kalthoff et al. (2011) over different orographic terrains. However, convection was predominantly initiated over mountain crests, independent of the instability indices, but with smaller convective inhibition (CIN). The dependency of equivalent potential temperature on soil moisture was found to be influenced by surface inhomogeneity. Barthlott and Kalthoff (2011) provide a sensitivity study in which the soil moisture was increased by $\pm$ 50% in steps of 5%. While a systematic effect on the 24 hours precipitation sum for reduced soil moisture exists, precipitation does not react systematically in wetter simulations.

Diversity in the results may partly be attributed to model uncertainty. Hohenegger and Schär (2007) investigated the error growth of random perturbation-methods in cloud-resolving models using time shifted model simulations and perturbed temperature fields in the initial conditions. In their model study, using a model resolution of $2.2\,\mathrm{km}$, a rapid error growth was found far away from the perturbed regions, but growth of uncertainties is limited by the large-scale atmospheric environment. A further aspect of model uncertainties is provided by the model resolution especially in terms of convection. Different results of soil moisture-precipitation feedback occur for simulations with explicit and differently parametrized convection (Hohenegger et al., 2009). Hohenegger et al. (2008) found different results in sign and strength of the influence of soil moisture that depended on the model resolution. Simulations with explicitly resolved convection indicate a negative soil moisture-precipitation feedback, that is in agreement with many other studies, summerised by Barthlott and Kalthoff (2011).

Soil moisture perturbations are directly assessed to generate an ensemble spread in numerical weather forecasts. Weather services include soil moisture perturbation in data assimilation for their ensemble forecast systems as MeteoSwiss does by using the method from Schraff et al. (2016) in the COSMO model to achieve a model spread especially in summer (pers. com. Daniel Leuenberger, MeteoSwiss). The evaluation of the AROME-EPS ensemble prediction system from Bouttier et al. (2016), which also includes soil moisture perturbations, showed that a lack in precipitation spread remains. That rises the question if soil moisture perturbations can cause sufficient differences in precipitation. This question will be addressed in the present study. As

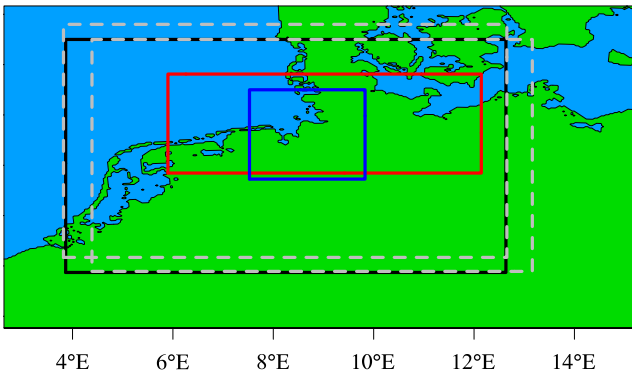


**Figure 1.** Model domain over Northern Germany given by the black rectangle for the CTRL run. Dashed gray rectangles describe the model domain, which is shifted by 30 gridpoints to the north and to the east, respectively. The two analysis areas are marked with red and blue rectangles.

Richard et al. (2007) already stated, convective precipitation output strongly depends on model setup, such as the prescribed initial conditions and boundary data. In the present study, we provide an uncertainty estimate that allows random changes in precipitation and changes that results from differences in soil moisture. With a uncertainty estimate, which is based on a large number of simulations with slightly different model setups, the effect of different soil moisture modifications on precipitation can be assessed and quantified. Furthermore, an effect caused by soil moisture can be separated from random changes. This determines if soil moisture perturbations can provide a sufficiently large ensemble spread for ensemble forecast.

Model simulations are conducted with the regional model COSMO (section 2.1). The soil moisture experiments and the ensemble approach are presented in sections 2.2 and 2.3, respectively for a single case with convective precipitation. An overview of the synoptic conditions for this convective case is provided in section 3. An estimate on the model uncertainty based on the CTRL-ensemble is calculated in section 4.2. With the given uncertainty range, the significance of soil moisture changes compared to the model spread is assessed in section 4.3, and systematics in the soil moisture impact are investigated in section 4.4.

## 2 Modelling approach

### 2.1 Numerical setup

We performed 24-hour simulations to simulate the convectively induced precipitation on 3 August 2012 over the area around Hamburg, using the non-hydrostatic model COSMO (Version 4.22, Schättler et al., 2009) with a horizontal resolution of 0.1° (≈1 km). The chosen domain covers 400 × 450 grid points over Northern Germany (Fig. 1). 50 vertical hybrid Gal-Chen levels range from the surface to a height of 22 km. The lowest level has a vertical resolution of 20 m. The boundary and initial conditions are provided by the COSMO operational analysis with a resolution of 2.8 km.

The horizontal resolution of around 1 km allows for an explicit representation of convection, and thus provides much more accurate simulations of convective precipitation than resolutions, which require convection parametrizations (Leutwyler et al., 2016, and references therein). Shallow convection is parametrized by the Tiedke Scheme (Tiedtke, 1989). Land surface processes are calculated by the interactive soil and vegetation model TERRA-ML and coupled to the atmospheric module (Doms et al., 2011). The coupled soil model includes seven soil levels from the surface to a depth of 14.58 m with the uppermost layer having a vertical extension of 5 mm.

### 2.2 Soil moisture experiments

To address the potential effect of soil moisture on precipitation, the soil moisture content provided in the initial conditions was modified (Table 1). Two classes of changes in the soil moisture field were applied: extreme artificial changes, which show a large range of soil moisture influence and modifications in a physically feasible range (Fig. 2). Among the strong modifications is the total drying of soil by setting the soil moisture content to zero (Fig. 2c). Soil moisture increase is achieved by an enhancement of 50% (Fig. 2d) in all soil layers. Those changes are applied first over the whole model domain ($DRY_a$ and $MOI_a$, Table 1, Fig. 1) and secondly over the red framed domain in Fig. 1, hereafter referred to as area "red" ($DRY_p$ and $MOI_p$, Table 1). Another artificial modification is achieved by a redistribution into four alternating bands with 50% enhanced and reduced soil moisture, respectively (Fig. 2b). A large range of possible soil moisture effects is covered with this modifications. More realistic, but slightly less intense, modifications are implemented by replacing the soil moisture pattern by one from another day (Fig. 2e). Therefore, the soil moisture field from 20 August 2012 is used (Fig. 3). On that day the soil moisture content in the uppermost soil layer (5 mm) is around 1.2 mm [$H_2O$] averaged over all land points, what is 0.3 mm lower than on the simulated day (3 August 2012). On 19 July 2012 soil moisture content was slightly below the 50%-artificial enhancement (Fig. 3). Therefore, the soil moisture was higher than on 3 August and thus this day was used to simulate 3 August 2012 with realistic, but higher soil moisture.

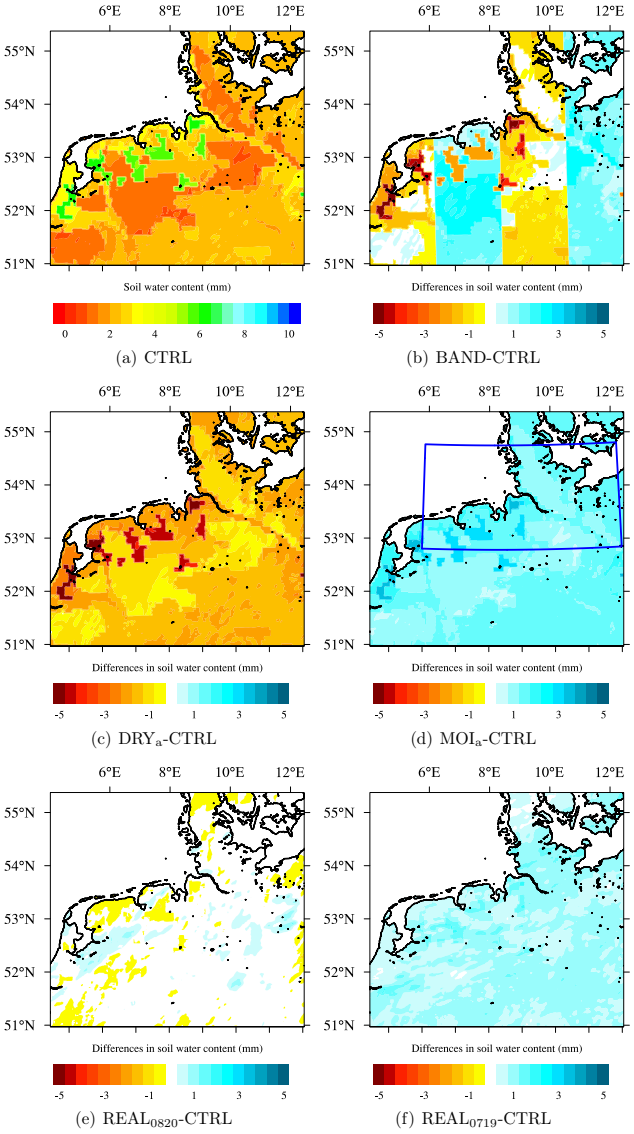


**Figure 2.** (a) Soil moisture for CTRL run and differences between CTRL run and (b) BAND run, (c) $\mathrm{DRY_a}$ run, (d) $\mathrm{MOI_a}$ run, (e) $\mathrm{REAL_{0820}}$ run and (f) $\mathrm{REAL_{0719}}$ run in the uppermost soil layer. Blue rectangle indicates the region where soil moisture was changed in $\mathrm{DRY_p}$ run and $\mathrm{MOI_p}$ run.

### 2.3 Ensemble approach

To quantify the relevance of the results from the soil moisture modifications, the model uncertainty and variability is estimated with a novel and simple approach. Perturbations are introduced by shifting the domain boundaries by ten to 30 grid points north- and eastwards (Table 2, Fig. 1). These perturbations provide an estimate of the uncertainty caused by the chaotic be-

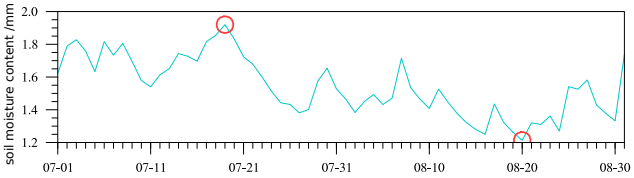


**Figure 3.** Time series for soil moisture content in the uppermost soil level averaged over the analysis domain "red". Red circles indicate the soil moisture values, which were used to perform simulations with soil moisture from another day.

**Table 1.** Model simulations with modified soil moisture (SM). Simulations are named by the applied soil moisture modification and with $a$ for whole model domain and $p$ for modification in a subdomain (partly). Simulations with additional random changes are denoted with $ii$ and $jj$, which represents number of gridpoints by which the model domain is shifted (For details see Table 2).

| reference simulation for ensemble | Characteristics | | ensemble generation | |
|---|---|---|---|---|
| | modification | area | | |
| CTRL | | | CTRL-LOC*ii jj* | TIME*tt* |
| $DRY_a$ | dry out | whole model domain | $DRY_a$-LOC*ii jj* | |
| $DRY_p$ | dry out | area “red” | $DRY_p$-LOC*ii jj* | |
| $MOI_a$ | 50% increased SM | whole model domain | $MOI_a$-LOC*ii jj* | |
| $MOI_p$ | 50% increased SM | area “red” | $MOI_p$-LOC*ii jj* | |
| BAND | four bands | whole model domain | BAND-LOC*ii jj* | |
| $REAL_{0820}$ | SM from 20.08.12 | whole model domain | $REAL_{0820}$-LOC*ii jj* | |
| $REAL_{0719}$ | SM from 19.07.12 | whole model domain | $REAL_{0719}$-LOC*ii jj* | |

haviour of the atmospheric system and are superimposed on all systematic and physical changes caused by the soil moisture perturbations. This method conserves the structure of all meteorological input fields and does not create errors on a scale that can interact with the analysed processes eg by creating small scale secondary circulation. Furthermore, shifting start times of the simulations (Hohenegger and Schär, 2007) provide an additional degree of uncertainty. A time shift of one to six hours is also applied to the CTRL run to fairly compare uncertainty estimates. The ensemble, further called the CTRL-ensemble, delivers 17 independent model simulations including the reference simulation (CTRL-run) to estimate the uncertainty. The ensemble approach, including all simulations with shifted model domains, was applied on every simulation with the modified soil moisture pattern (Table 2).

**Table 2.** Uncertainty-ensemble with randomly changed model simulations by model domain shifting, denoted with LOC and the number of shifted grid points, and by shifting the model start time denoted with TIME. The shifted time is given in hours. The lower left (LL) corner of the simulation domains is given in geographical (rotated) coordinates with the north pole being shifted to 40° N and -170° E.

| run | LL corner in ° N | LL corner in ° E | starttime (UTC) |
|---|---|---|---|
| CTRL | 50.87 (1.0) | 15.55 (3.5) | 0:00 |
| LOC 00 10 | 50.97 (1.1) | 15.56 (3.5) | 0:00 |
| LOC 00 20 | 51.07 (1.2) | 15.57 (3.5) | 0:00 |
| LOC 00 30 | 51.17 (1.3) | 15.59 (3.5) | 0:00 |
| LOC 10 00 | 50.88 (1.0) | 15.39 (3.4) | 0:00 |
| LOC 10 10 | 50.98 (1.1) | 15.40 (3.4) | 0:00 |
| LOC 10 20 | 51.08 (1.2) | 15.42 (3.4) | 0:00 |
| LOC 20 00 | 50.89 (1.0) | 15.23 (3.3) | 0:00 |
| LOC 20 10 | 50.98 (1.1) | 15.25 (3.3) | 0:00 |
| LOC 20 20 | 51.08 (1.2) | 15.26 (3.3) | 0:00 |
| LOC 30 00 | 50.89 (1.0) | 15.08 (3.2) | 0:00 |
| TIME 01 | 50.87 (1.0) | 15.55 (3.5) | 1:00 |
| TIME 02 | 50.87 (1.0) | 15.55 (3.5) | 2:00 |
| TIME 03 | 50.87 (1.0) | 15.55 (3.5) | 3:00 |
| TIME 04 | 50.87 (1.0) | 15.55 (3.5) | 4:00 |
| TIME 05 | 50.87 (1.0) | 15.55 (3.5) | 5:00 |
| TIME 06 | 50.87 (1.0) | 15.55 (3.5) | 6:00 |

## 3 Convective case-study and the effect of soil moisture

The chosen convective case on 3 August 2012 was affected by a low pressure system in the north Atlantic, west of Great Britain (Fig. 4). The associated cold front passed over Germany and resulted in heavy precipitation over Poland where air masses converged. Next to the major precipitation events in the east, another local precipitation cell developed close to Hamburg where a slight enhancement in convective available potential energy (CAPE)-values and high clouds occurred (Fig. 4). This locally strong precipitation was detected by the rain radars over Hamburg at 14:11 UTC with rain rates between 10 to 100 $\mathrm{mm\,h^{-1}}$ (Fig. 5). The simulations showed maximal values of 12 $\mathrm{mm\,h^{-1}}$ between 13:00 to 17:00 UTC. The simulated precipitation onset is at around 10:00 UTC (Fig. 6a). Before the precipitation onset, high CAPE-value confirms the convective nature of the precipitation (Fig. 6b). High CAPE-values enable strong convective precipitation formation, when CIN can be exceeded.

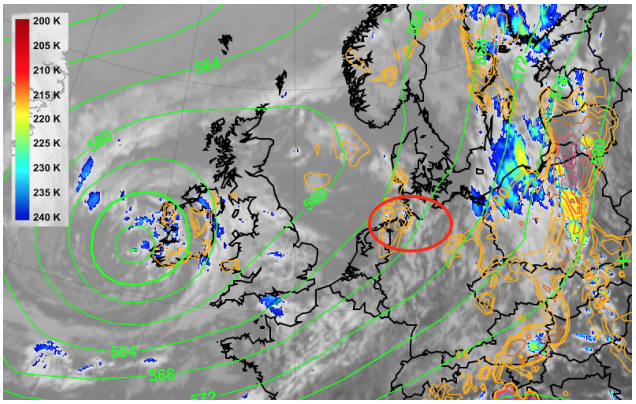


**Figure 4.** EUMEtrain infra-red satellite image of Europe on 3 August 2012 at 12:00 UTC. Colours are cloud top temperatures showing high clouds. Green contours are geopotential height at 500 hPa and orange contour lines are CAPE-values provided from ECMWF NWP (www.eumetrain.org). The area of interest is marked with a red circle. Note the CAPE values within the marked area and the high clouds, which correspond to the intense precipitation.

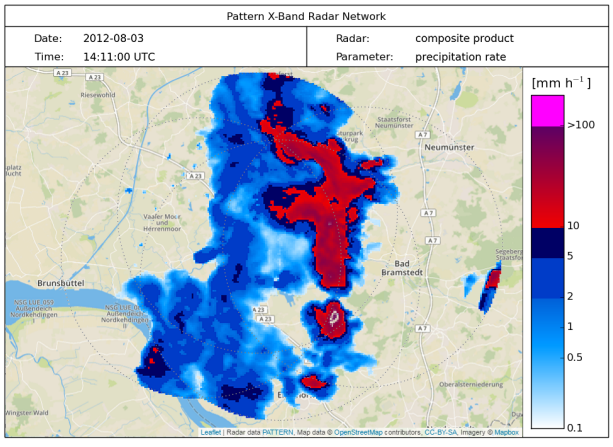


**Figure 5.** Radar composite from high resolution radars (Lengfeld et al., 2014) showing the precipitation rate over Itzehoe on 3 August 2012 at 14:11 UTC.

## 4 Results

### 4.1 Soil moisture influence on convective related variables

While the passing front stated the main mechanism for the lifting of air masses, soil moisture is important for the stability of the atmosphere and thus affecting the precipitation, which initially was triggered by the synoptic system. In complete dry conditions ($\mathrm{DRY_a}$ and $\mathrm{DRY_p}$), no latent heat fluxes transport heat from the surface. Thus, sensible heat fluxes need to balance the heat differences between surface and atmosphere (Fig. 7). Without latent cooling, the temperatures at $2\,\mathrm{m}$ altitude in the simulation with dry soil conditions ($\mathrm{DRY_a}$ and $\mathrm{DRY_p}$) are the highest, whereas dew point is the lowest (Fig. 7c and d). With more humidity in the atmosphere, less adiabatic cooling due to lifting is required for condensation. The resulting shift in the condensation level to lower altitudes can reduce CIN and increase CAPE. CIN only reduces in the first hours of the simulation before solar radiation heats the surface (Fig. 7). When the surface heats up, in simulations with low soil moisture content, CIN values are continuously lower than in simulations with higher soil moisture content. The further development of CIN is strongly affected by the feedback from precipitation.

All mentioned quantities react systematically on changes in soil moisture (Fig. 7). Convective precipitation is more likely with reduced CIN and its strength depends on CAPE. However, the changes in precipitation amount does not systematically react on the soil moisture. The main reason in literature for this systematic behaviour is due to the CIN dependency on the soil moisture (Kalthoff et al., 2011). Even though the changes in precipitation with changing soil moisture are more complex, precipitation is influenced by the soil moisture. However, that the changes in precipitation caused by soil moisture changes compared to the synoptic forcing are less significant will be shown in the following sections.

### 4.2 Estimate of model uncertainties

An estimate of the model uncertainty is determined from the CTRL-ensemble. The statistical tool, which was applied for this purpose, is the SAL-score (Wernli et al., 2008), which assigns values for differences in structure, $S$, amplitude, $A$ and location, $L$, of precipitation patterns at every single output-timestep (15 min).

Amplitude $A$ yields the differences of precipitation amount over the whole analysed domain:

$$A = \frac{D(R_{\mathrm{dif}}) - D(R_{\mathrm{ctrl}})}{0.5[D(R_{\mathrm{dif}}) + D(R_{\mathrm{ctrl}})]} \tag{1}$$

with the averaged precipitation amount, $D(R)$, for shifted simulation from the CTRL-ensemble denoted with $\mathrm{dif}$ and the compared simulation that is the not shifted reference simulation from the CTRL-ensemble denoted with $\mathrm{ctrl}$:

$$D(R) = \frac{1}{N_{\mathrm{GP}}} \sum_{(\mathrm{i,j})\in\epsilon} R_{\mathrm{ij}} \tag{2}$$

with the precipitation rate, $R_{\mathrm{ij}}$, within a grid point that is given by the indices, $\mathrm{i,j}$, and the number of all grid points, $N_{\mathrm{GP}}$, in the analysed domain.

Component location, $L$, compares the location of precipitation in the two model simulations in two steps. First, the normalised

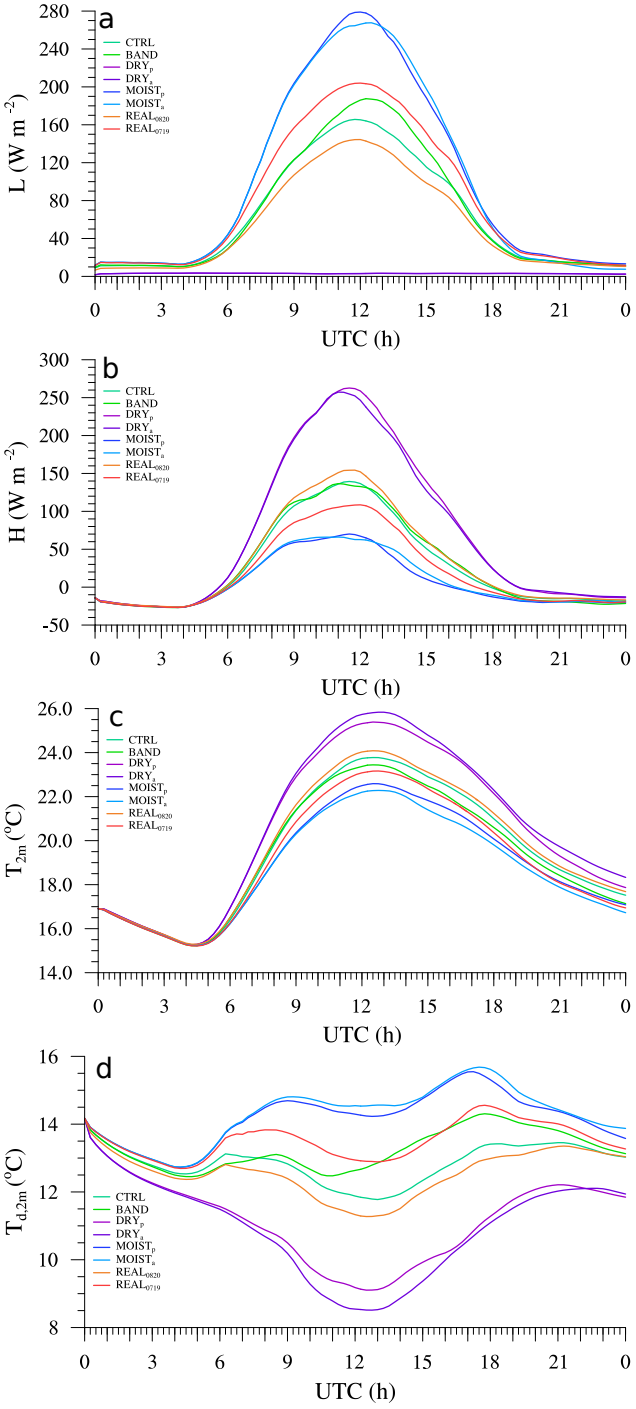


**Figure 6.** Timeseries of (a) latent heat fluxes, $L$, (b) sensible heat fluxes, $H$, (c) 2m-temperature and (d) dew point temperature, $T_{\mathrm{d}}$ in the reference simulations of the ensembles with different soil moisture modifications for 3 August 2013. Averaged over area red.

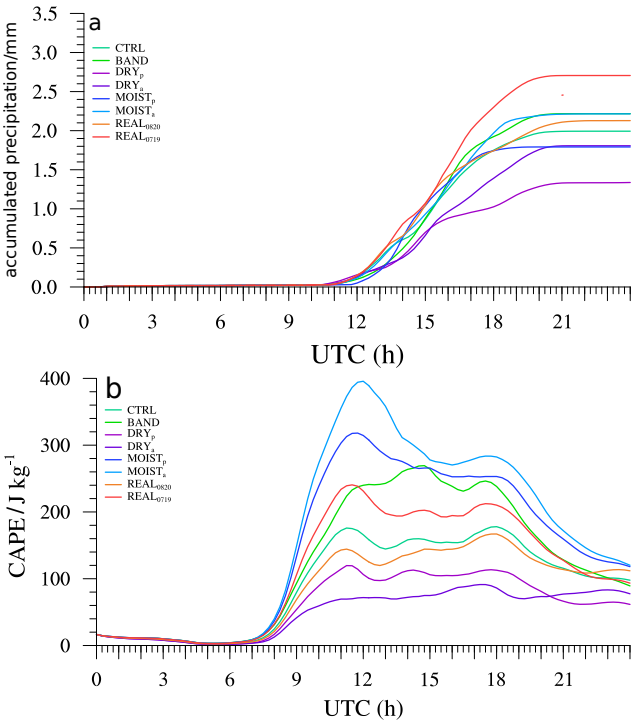


**Figure 7.** Timeseries of (a) accumulated precipitation and (b) CAPE for different model simulations for 3 August 2013. Averaged over red area.

distance of the centres of mass, $\mathbf{x}(R)$, of the precipitation patterns in each model simulation is calculated.

$$L_1 = \frac{|\mathbf{x}(R_{\mathrm{dif}}) - \mathbf{x}(R_{\mathrm{ctrl}})|}{d}, \tag{3}$$

where $d$ denotes the maximal distance within the analysed domain.

Secondly the distances from the centre of mass of all, $M$, individual cells, $\mathbf{x}_n$, to the centre of mass for the whole precipitation field, $\mathbf{x}$, is calculated:

$$r(R) = \frac{\sum_{n=1}^{M} R_n \, |\mathbf{x} - \mathbf{x}_n|}{\sum_{n=1}^{M} R_n} \tag{4}$$

and compared:

$$L_2 = 2 \left[ \frac{|r(R_{\mathrm{dif}}) - r(R_{\mathrm{ctrl}})|}{d} \right]. \tag{5}$$

Both components of $L$ are added.

Structure component, $S$, gives a hint whether the precipitation patterns tend to more convective precipitation with small but more peaked rain objects or shallow precipitation with larger but less precipitating objects. Therefore, a volume, $V(R)$, is calculated by the sum of precipitation, $\mathcal{R}_{ij}$, over all grid cells, $\epsilon$, within a precipitation cell, $n$, and the maximal precipitation,

$R_n^{max}$, within this cell:

$$V_n = \sum_{(\mathrm{i,j})\in\epsilon} \frac{\mathcal{R}_{\mathrm{ij}}}{R_n^{max}}, \tag{6}$$

$$V(R) = \frac{\sum_{n=1}^{M} R_n V_n}{\sum_{n=1}^{M} R_n}. \tag{7}$$

With the volume, $V(R)$, over all precipitation cells, $M$, the structure component can be calculated similar to Eq. (1):

$$S = \frac{V(R_{\mathrm{dif}}) - V(R_{\mathrm{ctrl}})}{0.5[V(R_{\mathrm{dif}}) + V(R_{\mathrm{ctrl}})]}. \tag{8}$$

For more detailed information on SAL see Wernli et al. (2008).

The numerous simulations were compared in the time range from 10:00 UTC and 18:00 UTC, covering the precipitation event. Those with a shifted model start are compared to the CTRL run. Positive or negative amplitudes arise as an effect of which simulation is used as the reference run, denoted with ctrl or comparison run, denoted with dif. To avoid an uncertainty range tending more to one direction, all comparisons are done in reverse additionally, providing a symmetric uncertainty distribution. The uncertainty estimate (Fig. 8) encompasses a sample of 122 (permutation of simulation couples) $\times$ 32 (time steps) values, although they are not all independent of each other.

A and S are correlated (Fig. 8). Hence a reduction in precipitation amplitude is related to too small and/or peaked precipitation objects, whereas an increase in precipitation goes along with larger and/or shallower rain objects. The largest deviations arise in the first hours from 10:00 to 11:30 UTC of the analysis time (Fig. 9). This agrees with the beginning of the precipitation event in the different simulations because the onset of precipitation differs in all simulations (Fig. 6) and therefore causes the largest uncertainties. The end of the precipitation event is not considered in the chosen time range.

A large shift in model start time leads to higher uncertainties (Fig. 9). Changes due to the shifted model domain do not depend on the distance of the boundary shift. The deviations from CTRL for simulations with shifted boundaries are not caused by a direct change of physical parameters such as temperature in a first instance but the differences emerge because synoptic systems, such as low pressure systems, are included in the model boundaries differently. Differences are further caused by changes in the lower boundaries such as including a larger area of sea- or landcover. For example, a model domain with north- or westward shifted boundaries includes more grid points over sea surface. The simulation with the strongest westward shift (LOC3000) causes the largest changes in precipitation amplitude (Fig. 9), whereas the strongest northward shift by 30 km (LOC3000), which also includes a larger fraction of sea surface, affects precipitation amplitude less strongly than a shifting by 20 km north (LOC2000) (Fig. 9).

To address the dependency of SAL-score on the chosen analysis area, two different analysis areas are chosen (Fig. 1). The blue framed area in Fig. 1 includes mainly the small convective cells and the red framed area includes the whole precipitation field. For those two analysis areas two simulations are compared to each other respectively. We define the model uncertainty for this study as the range from 5% percentile to 95% percentile for structure and amplitude and by 90% percentile for location. According to this definition, the uncertainty range is $\pm 0.77$ ($\pm 0.86$) in structure, $\pm 0.54$ ($\pm 0.69$) in amplitude, and up to 0.20

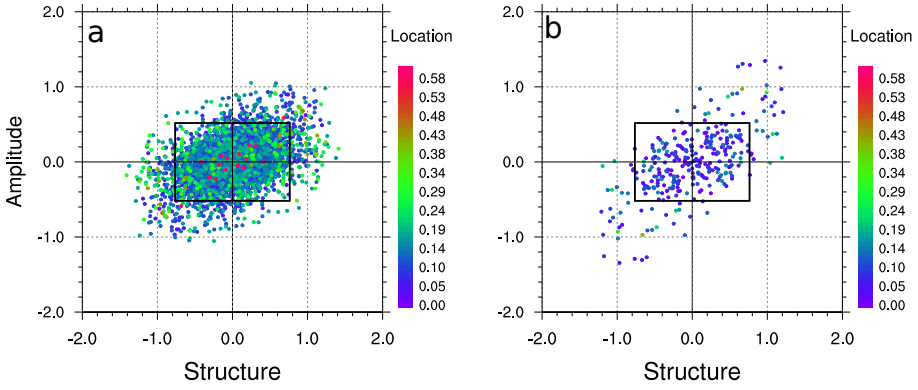


**Figure 8.** SAL results for the CTRL-uncertainty-ensemble between 10:00 UTC and 18:00 UTC separated for uncertainties generated by the shifted model domain (a) and by the delayed model start (b). Structure is represented on the x-axis, amplitude on y-axis and location by marker colours. Every marker presents a comparison between two model simulations at a single time step. Simulations with shifted model domain are presented by filled dots and those with shifted model start time by rectangles. The borders of the grey rectangle are calculated by 5% and 95% percentile of structure and amplitude.

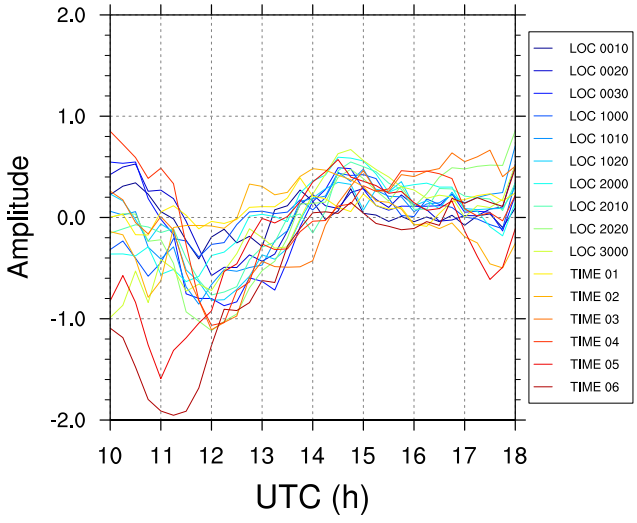


**Figure 9.** Amplitude values from Fig. 8 for comparisons to the CTRL run only on the single time steps.

(0.29) for analysis area “red” (“blue”). Changes are defined as significant when the response to the soil moisture modification is larger than the generated background noise. A residual probability of 10% remains that the latter are not a result of soil moisture modification. In comparison between the CTRL run (Fig. 10a) and the simulation with shifted boundaries (Fig. 10b), differences in the single cells in the West, partly over the North Sea, and in the structure of the large precipitation pattern in the East become obvious. These differences are caused by shifting the boundary domain by ten grid points (10 km). The extreme modifications in soil moisture cause even more obvious differences in the precipitation patterns. The enhancement of

soil moisture in either the whole domain or a sub domain changes the location of the precipitation for the chosen time dramatically (Fig. 10e and f). In the moist simulations ($MOI_a$ and $MOI_p$), the strongest precipitation occures north-east of the estuary. This region is mainly free of precipitation in the dry simulations ($DRY_a$ and $DRY_p$) and in the CTRL simulations (CTRL and LOC1000) the precipitation occurs even further north-east of this particular region. Moderate changes in soil moisture, such as applied by using realistic moisture fields, result in smaller changes in precipitation. The general pattern observed in the CTRL run remains in $REAL_{0820}$ and $REAL_{0719}$ (Fig. 10f and g).

### 4.3 Significant effects of soil moisture modification on precipitation

The huge number of model simulations (a complete ensemble for each soil moisture modification) and the uncertainty estimate from Sect. 4.2 accounts for a quantitative evaluation of the significance of soil moisture influence on precipitation.

Each ensemble with modified soil moisture will be compared to the CTRL-uncertainty ensemble by comparing ensemble members with the same shift of the model domain for every output-step. Within every ensemble the values are divided into those that exceed the uncertainty range (blue rectangle in Fig. 11) what is given by the uncertainty-ensemble, and those that are within. The percentage of the values exceeding the uncertainty range is calculated to decide whether a soil moisture modification leads to significant changes in precipitation (Table 3). Changes caused by a soil moisture modification will be treated as significant if more than 10% of the values exceed the uncertainty range. The threshold is set to 10% because the uncertainty range was calculated by the 5% and 95% what remains a 10% probability that an exceeding value can still be caused by model uncertainties.

The structural change of precipitation on soil moisture modification as in the $DRY_p$-ensemble exceeds the uncertainty in only 5% of all cases (Fig. 11a and Table 3). For both scores, S and A, the percentage of exceeding values lies beneath the 10% threshold. Therefore, precipitation does not respond significantly to $DRY_p$ modifications, but for L in area "red" (Table 3). In contrast, the soil moisture reduction in the whole domain ($DRY_a$-ensemble) affects the precipitation significantly (Fig. 11b). More than 50% of A exceed the uncertainty range in some cases with values for A down to -1.8. For S only 11% of the values exceed the range. Nevertheless, this is enough to be treated as a significant impact. The soil moisture enhancement in a sub domain only ($MOI_p$-ensemble), results in significant changes in precipitation (Fig. 11c). As already seen for the $DRY_a$-ensemble, the modification over the whole domain results in a stronger precipitation response.

The redistribution of soil moisture (BAND-ensemble) does not lead to any significant effect (Fig. 11e), except for L in area "blue". The redistribution of soil moisture changes the heterogeneity of the soil moisture by reducing small-scale structures, but induce stronger variations on a large scale. Thus, secondary circulation can develop on a different scale. This is in accordance with Adler et al. (2011); Kang and Bryan (2011) who found an influence of redistribution of soil moisture on the location of convective initiation. Therefore, area "blue", mainly containing small convective cells, is more influenced than area "red" with the large advected precipitation band.

Even slight modifications of soil moisture, as Klüpfel et al. (2011) performed by using different initialisations of soil moisture, lead to different precipitation patterns. Using soil moisture from another day also changes precipitation. But those changes do

**Table 3.** Percentages ($p_S, p_A, p_L$) of values S, A and L that exceed the model uncertainty by 90%. Uncertainties are in a range from $[-0.767, 0.767]([-0.857, 0.857])$ in structure, $[-0.538, 0.538]([-0.690, 0.690])$ in amplitude and $0.200(0.288)$ in location for analysis area "red" ("blue"). Bold values exceed model uncertainties in more than 10%. Averaged values and its deviation ($\overline{S} \pm \hat{\sigma}^2$, $\overline{A} \pm \hat{\sigma}^2$). Bold values are those mean values that differ significantly from the mean of the uncertainty-ensemble after Eq. (9) for confidence interval of 90%.

| Ensemble | Structure | | Amplitude | | Location |
|---|---|---|---|---|---|
| | $p_S$ | $\overline{S} \pm \hat{\sigma}^2$ | $p_A$ | $\overline{A} \pm \hat{\sigma}^2$ | $p_L$ |
| analysis area "red" | | | | | |
| $\mathrm{DRY_p}$ | 5.79 | $0.02 \pm 0.0034$ | 3.58 | $\mathbf{-0.13 \pm 0.0011}$ | **25.34** |
| $\mathrm{DRY_a}$ | **23.14** | $\mathbf{0.30 \pm 0.0063}$ | **22.31** | $\mathbf{-0.26 \pm 0.0023}$ | **53.72** |
| $\mathrm{MOI_p}$ | **15.98** | $-0.12 \pm 0.0051$ | **18.73** | $-0.05 \pm 0.0042$ | 8.26 |
| $\mathrm{MOI_a}$ | 9.92 | $-0.10 \pm 0.0043$ | **23.42** | $\mathbf{-0.18 \pm 0.0043}$ | **26.72** |
| BAND | 3.03 | $-0.04 \pm 0.0025$ | 0.55 | $0.00 \pm 0.0001$ | 6.61 |
| $\mathrm{REAL_{0820}}$ | 3.31 | $-0.03 \pm 0.0022$ | 0.28 | $-0.02 \pm 0.0006$ | 0.55 |
| $\mathrm{REAL_{0719}}$ | 2.48 | $0.05 \pm 0.0024$ | 1.65 | $0.09 \pm 0.0008$ | 1.65 |
| analysis area "blue" | | | | | |
| $\mathrm{DRY_p}$ | 4.85 | $-0.10 \pm 0.0033$ | 9.39 | $\mathbf{-0.29 \pm 0.0091}$ | 5.76 |
| $\mathrm{DRY_a}$ | **11.82** | $0.08 \pm 0.0058$ | **51.21** | $\mathbf{-0.60 \pm 0.0068}$ | **30.61** |
| $\mathrm{MOI_p}$ | **14.85** | $-0.19 \pm 0.0053$ | **12.12** | $0.00 \pm 0.0039$ | **12.42** |
| $\mathrm{MOI_a}$ | **15.76** | $\mathbf{-0.27 \pm 0.0058}$ | **19.70** | $\mathbf{-0.28 \pm 0.0044}$ | **27.58** |
| BAND | 7.27 | $-0.10 \pm 0.0045$ | 0.91 | $0.07 \pm 0.0014$ | **21.52** |
| $\mathrm{REAL_{0820}}$ | 0.91 | $-0.04 \pm 0.0026$ | 0.30 | $-0.03 \pm 0.0007$ | 1.21 |
| $\mathrm{REAL_{0719}}$ | 1.21 | $-0.01 \pm 0.0026$ | 0.30 | $0.07 \pm 0.0010$ | 1.21 |

not exceed the model uncertainty in more than 10% of all values in the present case. Accordingly, physically feasible changes in soil moisture lead to changes in precipitation not larger than changes that can also be caused by choosing a slightly different model setup.

### 4.4 Systematics

After determining the significance of the strength of changes in precipitation, this section handles the systematics of changes. Significant changes do not necessarily imply systematic changes. While in $\mathrm{DRY_a}$ (Fig. 11b) predominantly negative amplitude changes occur, in $\mathrm{MOI_p}$ (Fig. 11c) significant, but random changes occur. Structure and amplitude change in both positive and negative directions. In none of the soil moisture experiments S and A are correlated (Fig. 11). To carve out any systematic effects the averaged value of amplitude and structure are compared to the average of the uncertainty-ensemble. Systematics in L are not analysed as this quantity provides no direction. The sample for the SAL results for the uncertainty-ensemble is symmetric and therefore the average is zero. A significant difference of the averaged values from zero hints at the systematics.

Whether the averaged values differ significantly from zero is tested statistically by:

$$\widehat{z}_{\mathrm{sys}} = \frac{\overline{x}_1 - \overline{x}_2 - E[\overline{x}_1 - \overline{x}_2]}{\sqrt{\hat{\sigma}^2[\overline{x}_1 - \overline{x}_2]}}. \tag{9}$$

$\overline{x}_1$ and $\overline{x}_2$ denotes the averaged values of S or A for the two compared simulations, $E[\overline{x}_1 - \overline{x}_2]$ is the expected value for the differences between the two simulations and is expected to be zero for the null hypothesis, $\hat{\sigma}^2[\overline{x}_1 - \overline{x}_2]$ is the variance of averages.

The averaged structure differs significantly from zero only for the ensemble $\mathrm{DRY_a}$ and $\mathrm{MOI_a}$ by analysing over area red and blue respectively (Table 3). The amplitude reacts more often systematically in the analysis for both regions. Modifications of soil moisture by increasing and decreasing result both in reduced precipitation rates. This implies negative and positive feedbacks, respectively. The positive feedback, by decreasing the soil moisture, is in consent with Barthlott and Kalthoff (2011). The case study from Barthlott and Kalthoff (2011) shows a positive feedback for decreased soil moisture. But, enhanced soil moisture can lead to an increase or decrease in precipitation, dependent on the strength of soil moisture enhancement. In contrast, Cheng and Cotton (2004); Ek and Holtslag (2004); Martin and Xue (2006); Hohenegger et al. (2009); Weverberg et al. (2010) found a negative feedback in convection resolving simulations.

The strength of deviation depends on the strength of modification. While a partly increased soil moisture does not lead to systematic changes the overall enhancement has a systematic effect. The effect of dry soil exceeds the effect of soil moisture enhancement and shows systematic effects for both implementations. The effects are stronger for overall modifications. Comparing the results for both regions the averaged differences calculated for region "blue" exceed those of region "red" because convective cells are more influenced by soil moisture changes.

## 5 Conclusions

In the present case study we conducted seven ensembles of simulations with different perturbations in soil moisture. The letter include strong artificial changes and changes in a feasible range by replacing with real soil moisture patterns from another day. The ensembles were conducted over slightly different model domains, which were shifted 10 to 30 km to each other to deliver slightly changed boundary conditions. That caused a large spread in the convective case because the day (3 August 2012) was synoptically forced by a low pressure system over the Atlantic. Conclusively, only in two ensembles soil moisture caused significant changes in intensity, local distribution and amount of convective precipitation what was assessed with the SAL-score. The amplitude, determining a difference in amount of precipitation, is most often systematically reduced within an ensemble. Thus, no overall systematic was found because wetting and drying of soil result in reduced precipitation amount. The structure, which describes the difference in intensity in precipitation, can be either enhanced or decreased at different times and in different ensemble members what can also be caused by a time delay caused by soil moisture modification. A local displacement in the precipitation cells is found for three and four out of five artificially changed soil moisture patterns in the two different analysis regions, respectively. The changes in precipitation for the simulations with realistic soil moisture patterns are not significant.

Limitations in the present study are 1) the restriction to a single case study. Thus, no general valid results could be found. However, this study presents a proof of concept and can be conducted with further cases, which are less affected by frontal systems. In those cases a stronger influence of soil moisture can be expected. 2) The dependency of the results on the chosen analysis area, which in turn shows the complexity of the results. 3) The dependency of the uncertainty estimate on synoptic forcing and size of the model domain. The ensemble spread might become smaller with weaker synoptic forcing and with a larger model domain. However, a expected smaller model spread would strengthen the importance of soil moisture influence as it is expected in this cases.

In summary, we could proof the concept of shifting the model domain to achieve a sufficient large model spread without being influenced by generated patterns. Such an estimate of the model spread is necessary in soil moisture studies to assure the results from soil moisture changes. We further showed that under synoptically driven situation the effect of soil moisture remains uncertain and further investigations are necessary. To proceed the present study further cases studies should be conducted.

## References


Adler, B., Kalthoff, N., and Gantner, L.: The impact of soil moisture inhomogeneities on the modification of a mesoscale convective system: An idealised model study, Atmos. Res., 101, 354–372, doi:10.1016/j.atmosres.2011.03.013, 2011.

Barthlott, C. and Kalthoff, N.: A Numerical Sensitivity Study on the Impact of Soil Moisture on Convection-Related Parameters and Convective Precipitation over Complex Terrain, J. Atmos. Sci., 68, 2971–2987, doi:10.1175/JAS-D-11-027.1, 2011.

Barthlott, C., Hauck, C., Schädler, G., Kalthoff, N., and Kottmeier, C.: Soil moisture impacts on convective indices and precipitation over complex terrain, Meteorol. Z., 20, 185–197, doi:10.1127/0941-2948/2011/0216, 2011.

Bouttier, F., Raynaud, L., Nuissier, O., and Ménétrier, B.: Sensitivity of the AROME ensemble to initial and surface perturbations during HyMeX, Q. J. R. Meteorol. Soc., 142, 390–403, doi:10.1002/qj.2622, http://dx.doi.org/10.1002/qj.2622, 2016.

Cheng, W. Y. Y. and Cotton, W. R.: Sensitivity of a Cloud-Resolving Simulation of the Genesis of a Mesoscale Convective System to Horizontal Heterogeneities in Soil Moisture Initialization, J. Hydrometeor., 5, 934–958, doi:10.1175/1525-7541(2004)005<0934:SOACSO>2.0.CO;2, 2004.

Clark, D., Taylor, C., and Thorpe, A.: Feedback between the land surface and rainfall at convective length scales, J. Hydrometeor., 5, 625–639, doi:10.1175/1525-7541(2004)005<0625:FBTLSA>2.0.CO;2, 2004.

Dixon, N. S., Parker, D. J., Taylor, C. M., Garcia-Carreras, L., Harris, P. P., Marsham, J. H., Polcher, J., and Woolley, A.: The effect of background wind on mesoscale circulations above variable soil moisture in the Sahel, Q. J. R. Meteorol. Soc., 139, 1009–1024, 2013.

Doms, G., Förstner, J., Heise, E., Herzog, H.-J., Mironov, D., Raschendorfer, M., Reinhardt, T., Ritter, B., Schrodin, R., Schulz, J.-P., and Vogel, G.: A Description of the Nonhydrostatic Regional COSMO Model, Part 2: Physical Parameterization, Tech. rep., 2011.

Ek, M. B. and Holtslag, A. A. M.: Influence of Soil Moisture on Boundary Layer Cloud Development, J. Hydrometeor., 5, 86–99, doi:10.1175/1525-7541(2004)005<0086:IOSMOB>2.0.CO;2, 2004.

Froidevaux, P., Schlemmer, L., Schmidli, J., Langhans, W., and Schaer, C.: Influence of the Background Wind on the Local Soil Moisture-Precipitation Feedback, J. Atmos. Sci., 71, 782–799, doi:10.1175/JAS-D-13-0180.1, 2014.

Hauck, C., Barthlott, C., Krauss, L., and Kalthoff, N.: Soil moisture variability and its influence on convective precipitation over complex terrain, Q. J. R. Meteorol. Soc., 137, 42–56, doi:10.1002/qj.766, 2011.

Hohenegger, C. and Schär, C.: Predictability and error growth dynamics in cloud-resolving models, J. Atmos. Sci., 64, 4467–4478, doi:10.1175/2007JAS2143.1, 2007.

Hohenegger, C., Brockhaus, P., Bretherton, C. S., and Schär, C.: The soil moisture-precipitation feedback in simulations with explicit and parameterized convection, J. Clim., 22, 5003–5020, doi:10.1175/2009JCLI2604.1, 2009.

Hohenegger, C., Brockhaus, P., and Schaer, C.: Towards climate simulations at cloud-resolving scales, Meteorol. Z., 17, 383–394, doi:10.1127/0941-2948/2008/0303, 2008.

Kalthoff, N., Kohler, M., Barthlott, C., Adler, B., Mobbs, S. D., Corsmeier, U., Traeumner, K., Foken, T., Eigenmann, R., Krauss, L., Khodayar, S., and Di Girolamo, P.: The dependence of convection-related parameters on surface and boundary-layer conditions over complex terrain, Q. J. R. Meteorol. Soc., 137, 70–80, doi:10.1002/qj.686, 2011.

Kang, S.-K. and Bryan, G. H.: A Large-Eddy Simulation Study of Moist Convection Initiation over Heterogeneous Surface Fluxes, Mon. Weather Rev., 139, 2901–2917, doi:10.1175/MWR-D-10-05037.1, 2011.

Klüpfel, V., Kalthoff, N., Gantner, L., and Kottmeier, C.: Evaluation of soil moisture ensemble runs to estimate precipitation variability in convection-permitting model simulations for West Africa, Atmos. Res., 101, 178–193, doi:10.1016/j.atmosres.2011.02.008, 2011.

Lengfeld, K., Clemens, M., Münster, H., and Ament, F.: Performance of high-resolution X-band weather radar networks - The PATTERN example, Atmos. Meas. Tech., 7, 4151–4166, doi:10.5194/amt-7-4151-2014, 2014.

Leutwyler, D., Fuhrer, O., Lapillonne, X., Lüthi, D., and Schär, C.: Towards European-scale convection-resolving climate simulations with GPUs: a study with COSMO4.19, Geosci. Model Dev., 9, 3393–3412, doi:10.5194/gmd-9-3393-2016, 2016.

Maronga, B. and Raasch, S.: Large-Eddy Simulations of Surface Heterogeneity Effects on the Convective Boundary Layer During the LITFASS-2003 Experiment, Boundary-Layer Meteorol., 146, 17–44, doi:10.1007/s10546-012-9748-z, 2013.

Martin, W. J. and Xue, M.: Sensitivity analysis of convection of the 24 May 2002 IHOP case using very large ensembles, Mon. Weather Rev., 134, 192–207, doi:10.1007/11768012_21, 2006.

Mass, C. F., Ovens, D., Westrick, K., and Colle, B. A.: Does increasing horizontal resolution produce more skillful forecasts? The results of two years of real-time numerical weather prediction over the Pacific Northwest, Bull. Amer. Meteor. Soc., 83, 407–430+341, doi:10.1175/1520-0477(2002)083<0407:DIHRPM>2.3.CO;2, 2002.

Pedersen, L., Jensen, N. E., Christensen, L. E., and Madsen, H.: Quantification of the spatial variability of rainfall based on a dense network of rain gauges, Atmos. Res., 95, 441–454, doi:10.1016/j.atmosres.2009.11.007, http://dx.doi.org/10.1016/j.atmosres.2009.11.007, 2010.

Richard, E., Buzzi, A., and Zängl, G.: Quantitative precipitation forecasting in the Alps: The advances achieved by the Mesoscale Alpine Programme, Q. J. R. Meteorol. Soc., 133, 831–846, doi:10.1002/qj.65, 2007.

Schättler, U., G., D., and C., S.: A description of the nonhydrostatic regional COSMO model. Part VII: User's Guide, 2009.

Schraff, C., Reich, H., Rhodin, A., Schomburg, A., Stephan, K., Periáñez, A., and Potthast, R.: Kilometre-scale ensemble data assimilation for the COSMO model (KENDA), Q. J. R. Meteorol. Soc., 142, 1453–1472, doi:10.1002/qj.2748, http://dx.doi.org/10.1002/qj.2748, 2016.

Tiedtke, M.: A Comprehensive Mass Flux Scheme for Cumulus Parameterization in Large-Scale Models, Monthly Weather Review, 117, 1779–1800, doi:10.1175/1520-0493(1989)117<1779:ACMFSF>2.0.CO;2, https://doi.org/10.1175/1520-0493(1989)117<1779:ACMFSF>2.0.CO;2, 1989.

Wernli, H., Paulat, M., Hagen, M., and Frei, C.: SAL-A Novel Quality Measure for the Verification of Quantitative Precipitation Forecasts, Mon. Weather Rev., 136, 4470–4487, doi:10.1175/2008MWR2415.1, 2008.

Weverberg, K. V., van Lipzig, N. P. M., Delobbe, L., and Lauwaet, D.: Sensitivity of quantitative precipitation forecast to soil moisture initialization and microphysics parametrization, Q. J. R. Meteorol. Soc., 136, 978–996, doi:10.1002/qj.611, 2010.

## Data availability

Model output data are stored at DKRZ computers and can be provided on demand.

*Acknowledgements.* We would like to thank the COSMO consortium for access to the code, and the German weather service (DWD) for providing analysis data, Deutsches Klimarechenzentrum (DKRZ) for providing a simulation platform and Heini Wernli and Markus Zimmer for the SAL analysis code. Thanks to Will Ball for proofreading. We thank the anonymous reviewers for their fruitful comments to improve this manuscript.

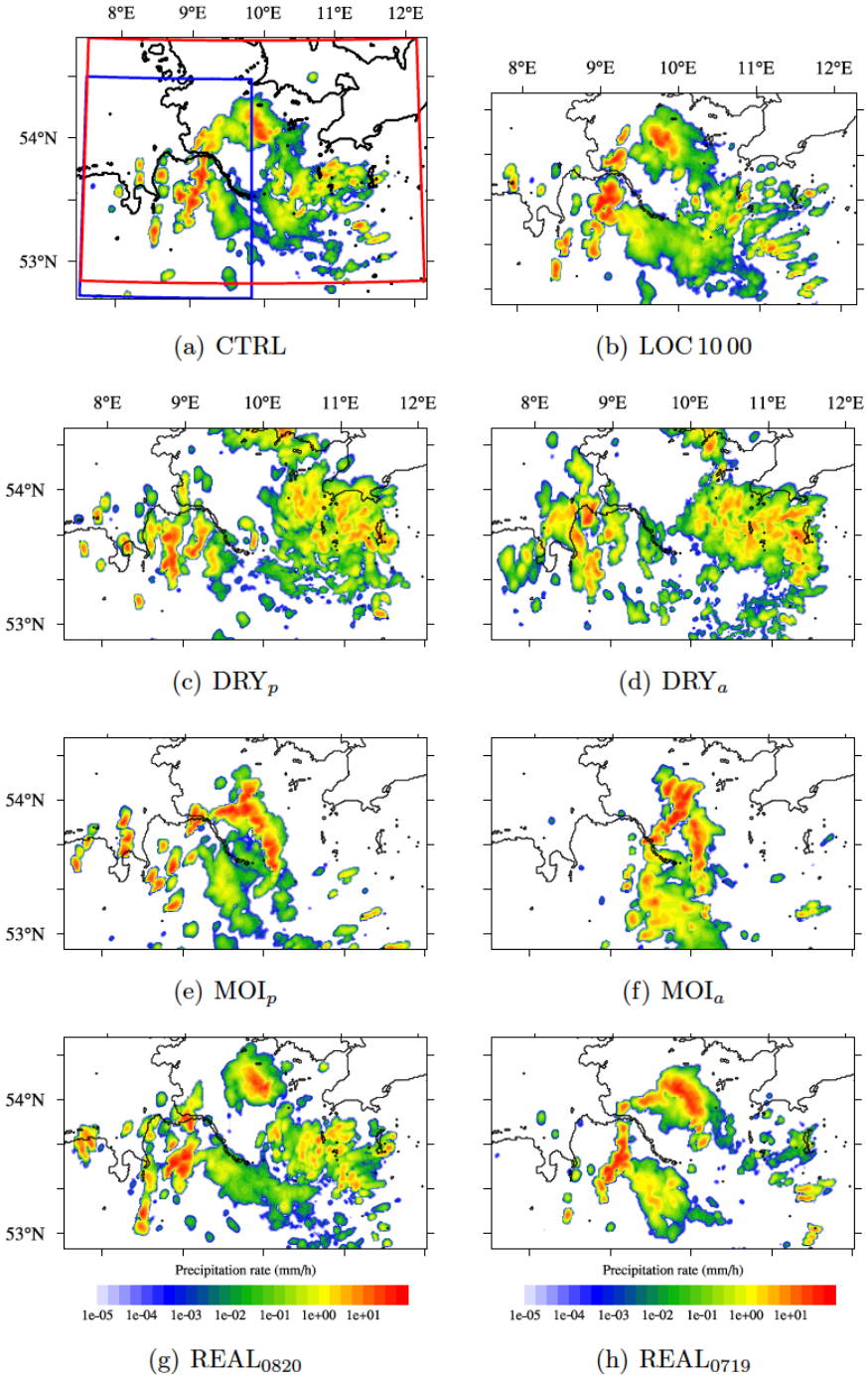


**Figure 10.** Precipitation rate at 14:45 UTC for (a) CTRL run , (b) LOC 10 00 and (c-h) different soil moisture modified simulations.

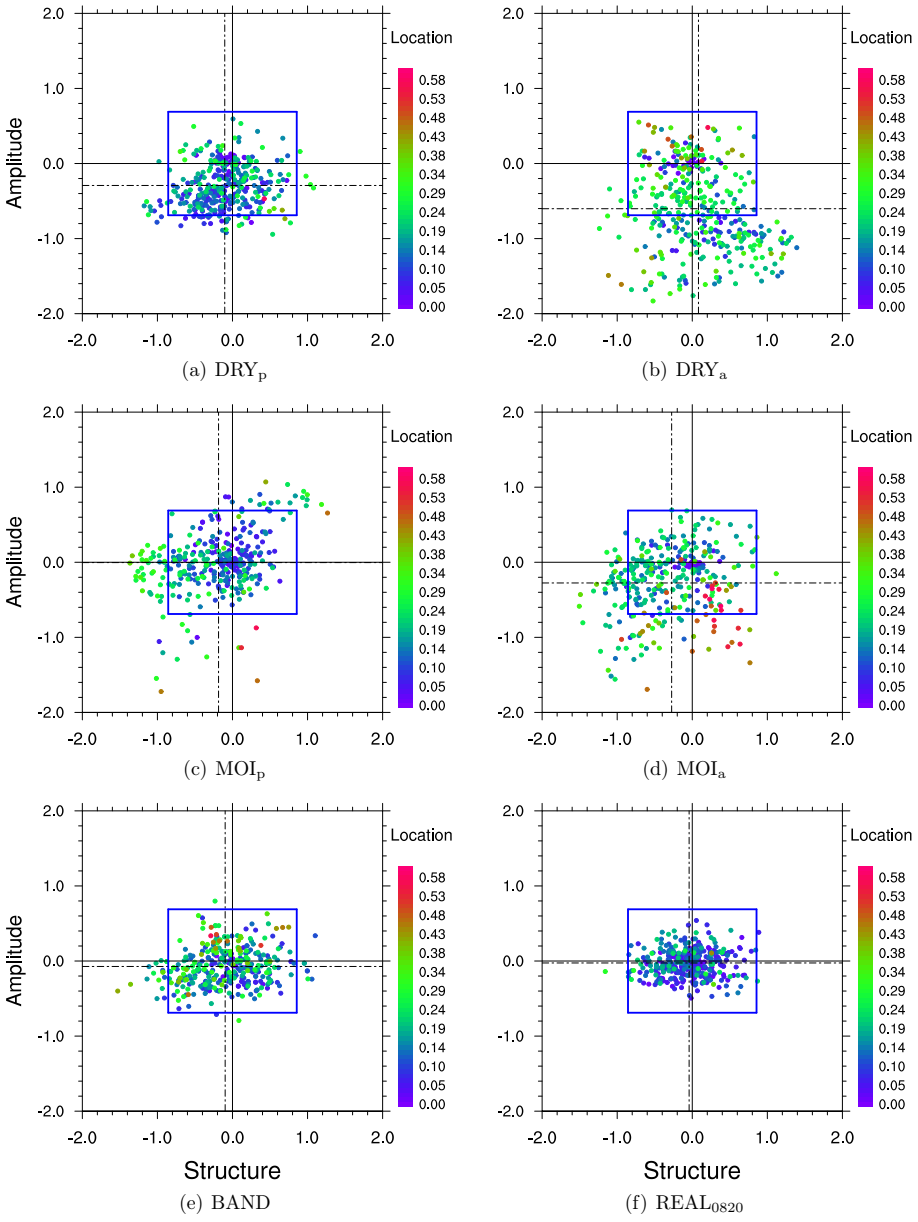


(a) $DRY_p$ (b) $DRY_a$

(c) $MOI_p$ (d) $MOI_a$

(e) BAND (f) $REAL_{0820}$

**Figure 11.** SAL scatter plot: Comparison of ensembles (a) $DRY_p$, (b) $DRY_a$, (c) $MOI_p$, (d) $MOI_a$, (e) BAND and (f) $MOI_{0820}$ with the uncertainty-ensemble for area "blue". Dashed lines represent the averages.